Fusion Engineering and Design 8 (1989) 257–264
North-Holland, Amsterdam

ANALYSIS OF LIQUID METAL MHD FLOW USING AN ITERATIVE METHOD TO SOLVE THE CORE FLOW EQUATIONS

K.A. McCARTHY, M.S. TILLACK and M.A. ABDOU

Mechanical, Aerospace and Nuclear Engineering Department, University of California, Los Angeles, Los Angeles, CA 90024-1597, USA

A computationally efficient and fast method for characterizing MHD fluid flow based on the "core flow" approximation is presented. The results of analysis of a number of practical problems that were solved using this method are also discussed.

At very high Hartmann number and interaction parameter and at very small magnetic Reynolds number, the equations describing the flow are essentially linear and are therefore solved more easily. By solving these equations, the three-dimensional characteristics of the flow can be examined using a two-dimensional computer code. The method used to solve these equations is an iterative one. A velocity profile is assumed and the equations are solved in a plane in the fluid. The equations are then solved in the domain of the duct wall. The potential in the wall is compared to the potential in the fluid along the magnetic field lines. If the variation of the potential along field lines is not correct, the velocities are adjusted. The potential distribution in the fluid can then be calculated again. This procedure is repeated until the variation of the potential along field lines is correct.

This method is applied to flow in a conducting duct with a transverse magnetic field that varies in the flow direction. The pressure drop dependence on various factors is discussed. The method appears to be particularly suited to problems with complex geometries, because the equations may not be as complicated as in the direct integration method. The results of the analysis are shown to compare well with experimental results.

1. Introduction

The self-cooled liquid metal blanket is a prime candidate for use in a fusion reactor. While lithium containing liquid metals have good heat transfer and tritium breeding characteristics, their flow is affected by the presence of a magnetic field. These magnetohydrodynamic (MHD) effects have an impact on heat transfer, mass transfer, and the pressure drop.

The set of equations describing MHD flow consists of the Navier–Stokes equation, Maxwell's equations, Ohm's law, and the mass conservation equation. The Navier–Stokes equation is nonlinear, and certain terms in it can be many orders of magnitude larger than other terms. For these reasons, the MHD equations are very difficult to solve analytically or numerically.

Straight conducting circular ducts with transverse magnetic fields that vary in the flow direction have been analyzed analytically using asymptotic methods [1]. While these methods are very good for predicting trends, in general, applicability to the fusion blanket is limited.

A numerical solution of the full set of equations would give the most accurate solution for any situation. But, as mentioned above, this is particularly difficult to do, especially at the high magnetic fields characteristic of a fusion reactor. There are cases, however, when certain terms can be neglected in the Navier–Stokes equation and Ampère's law, making the MHD equations linear and eliminating the difficulties associated with their numerical solution. When the magnetic field is high enough, viscous and inertial terms can often be neglected without a significant impact on the calculation of the core flow variables. In addition, if the induced magnetic field is negligible with respect to the applied magnetic field, the magnetic field can be assumed known. After making the simplifications implied by these assumptions, the set of MHD equations can be solved numerically without the problems inherent in the solution of the full set of equations.

Two methods of solving these equations have been explored. One is a "direct integration" method where the equations are integrated along magnetic field lines [2,3]. The resulting equations are then solved subject to the correct boundary conditions. While this method is applicable, in principle, to any problem, the equations become quite unwieldy in certain complex geometries.

An alternative method has been developed which avoids these complications. It is an iterative method – the full set of equations is not solved simultaneously. A velocity profile is assumed and the equations are solved in a plane in the fluid. The equations are then solved in the domain of the duct wall. The potentials in the wall and fluid are compared along magnetic field lines, and if they do not vary in a specified way, the velocity is modified. This process is repeated until the correct solution is found. Because the full set of equations is not integrated and combined, the equations being solved may not be as complex as those derived in the direct integration method. For this reason, the iterative method should be easier to apply to problems with complicated geometries.

2. Background information

The equations describing steady-state, incompressible MHD flow are

$$\rho \boldsymbol{v} \cdot \nabla \boldsymbol{v} = -\nabla p + \boldsymbol{j} \times \boldsymbol{B} + \mu \nabla^2 \boldsymbol{v}, \tag{1}$$

$$\boldsymbol{j} = \sigma(-\nabla \phi + \boldsymbol{v} \times \boldsymbol{B}), \tag{2}$$

$$\nabla \cdot \boldsymbol{B} = 0, \tag{3}$$

$$\nabla \times \boldsymbol{B} = \mu_0 \boldsymbol{j}, \tag{4}$$

$$\nabla \cdot \boldsymbol{v} = 0, \tag{5}$$

where ρ is the fluid density, $\boldsymbol{v}$ is velocity, p is pressure, $\boldsymbol{j}$ is current density, $\boldsymbol{B}$ is the magnetic field, μ is viscosity, σ is conductivity, and ϕ is potential. These equations can be nondimensionalized by setting $\boldsymbol{v}^* = \boldsymbol{v}/v$, $\boldsymbol{B}^* = \boldsymbol{B}/B_0$, $\boldsymbol{j}^* = \boldsymbol{j}/\sigma_f v B_0$, $\phi^* = \phi/avB_0$, and $p^* = p/\sigma_f v B^2 a$. In these relationships, the starred quantities are dimensionless, and v is the bulk velocity, B_0 is the maximum magnetic field, and a is the duct half-width.

The dimensionless MHD equations are (dropping the stars)

$$N^{-1} \boldsymbol{v} \cdot \nabla \boldsymbol{v} = -\nabla p + \boldsymbol{j} \times \boldsymbol{B} + M^{-2} \nabla^2 \boldsymbol{v}, \tag{6}$$

$$\boldsymbol{j} = -\nabla \phi + \boldsymbol{v} \times \boldsymbol{B}, \tag{7}$$

$$\nabla \cdot \boldsymbol{B} = 0, \tag{8}$$

$$\nabla \times \boldsymbol{B} = R_m \boldsymbol{j}, \tag{9}$$

$$\nabla \cdot \boldsymbol{v} = 0, \tag{10}$$

where N is the interaction parameter, $N = \sigma B^2 a/\rho v$, M is the Hartmann number, $M = Ba\sqrt{\sigma/\mu}$, and R_m is the magnetic Reynolds number, $R_m = \mu_0 \sigma v a$. The interaction parameter is the ratio of magnetic forces to inertial forces, the Hartmann number squared is the ratio of magnetic forces to viscous forces, and the magnetic Reynolds number is the ratio of the induced magnetic field to the applied magnetic field.

In order to make the solution of these equations easier, certain simplifications can be made. Inertial and viscous forces are important in the boundary and shear layers, while in the core flow they are generally negligible (see, for example, [4]). If the following assumptions are made:

(1) viscous forces are negligible ($M \to \infty$),

(2) inertial forces are negligible ($N \to \infty$),

(3) the induced magnetic field is negligible ($R_m \to 0$),

then the dimensionless equations governing steady, inertialess, inviscid MHD flow are

$$\nabla p = \boldsymbol{j} \times \boldsymbol{B}, \tag{11}$$

$$\boldsymbol{j} = -\nabla \phi + \boldsymbol{v} \times \boldsymbol{B}, \tag{12}$$

$$\nabla \cdot \boldsymbol{j} = 0, \tag{13}$$

$$\nabla \cdot \boldsymbol{v} = 0. \tag{14}$$

The flow is treated as if it is made up entirely of core flow. Because the induced magnetic field is assumed negligible, the magnetic field is known. The boundary layers are assumed to have a negligible effect on the core flow. This is usually a valid assumption as long as there is a component of the magnetic field perpendicular to the duct wall. If the magnetic field is parallel to the wall, the problem can still be treated, but special treatment of the boundary layers at these points must be made. In circular ducts with transverse magnetic fields, this is violated only at a point, so all boundary layers can be neglected.

3. Description of the iterative solution method

The iterative method alternatively solves a simplified set of equations in the fluid and in the wall. The duct and fluid are both mapped directly. When the equations and boundary conditions are satisfied in both regions, the problem is solved.

The equations are solved on a two-dimensional surface. By taking the curl of the Navier–Stokes equation, the variation of the current density along magnetic field lines can be determined. By taking the curl of Ohm's law, the variation of the velocity along magnetic field lines is found. Therefore, once the solution is known on a two-dimensional surface, the solution in the entire domain can be calculated.

In the domain of the fluid, the core flow equations are given by eqs. (11)–(14). After assuming a velocity field, ϕ and j can be determined using eqs. (12) and (13). Combining eqs. (12) and (13) yields

$$\nabla^2\phi = \nabla\cdot(\boldsymbol{v}\times\boldsymbol{B}). \tag{15}$$

By taking the curl of the Navier–Stokes equation, an expression for the variation of the current density, and thus the potential along field lines, is found. This expression is used in eq. (15) so that it can be solved in terms of x and y.

The potential distribution in the wall is calculated next. In the domain of the wall, Ohm's law and current conservation are used

$$j = -\frac{\sigma_w}{\sigma_f}\nabla\phi, \tag{16}$$

$$\nabla\cdot j = j_f\cdot n, \tag{17}$$

where n is a unit normal pointing from the wall to the fluid. Eqs. (16) and (17) can be combined, resulting in the following equation

$$\nabla^2\phi = -\frac{\sigma_f}{\sigma_w}j_f\cdot n, \tag{18}$$

where j_f is calculated from the potential distribution in the fluid using Ohm's law (eq. (12)).

Once the potential distribution in the fluid and wall has been calculated, it is necessary to determine whether the equations have been satisfied in the entire domain of the problem. The criterion for determining this is based on the variation of the potential along the field lines. The component of Ohm's law in the direction of the magnetic field is integrated along a magnetic field line

$$\int_{l_1}^{l_2} \mathrm{d}l\frac{\partial\phi}{\partial l} = \phi_{l_2} - \phi_{l_1} = -\int_{l_1}^{l_2}\mathrm{d}l\, j_{fl}. \tag{19}$$

Integration of this equation results in an expression for the variation of the potential along the magnetic field lines.

The potentials in the fluid and wall are compared along field lines. If the potentials do not meet this criterion to within a specified error, it is necessary to adjust the velocities. First, a new potential distribution is calculated by taking a linear combination of the old fluid potential and what the fluid potential would be if it varied correctly along field lines:

$$\phi_f^{new} = \rho_1\phi_f^{old} + \rho_2\left(\phi_{l_2} + \int_{l_1}^{l_2}\mathrm{d}l\, j_{fl}\right), \tag{20}$$

where $\rho_1 + \rho_2 = 1$. This new potential distribution is then used to calculate a new guess for the axial velocity by using Ohm's law.

The axial velocity calculated in the manner described previously will not necessarily satisfy global mass conservation. The velocity must be normalized such that

$$\int\int \mathrm{d}\boldsymbol{a}\, v_{axial} = \text{constant}, \tag{21}$$

where **a** is the cross-sectional area of the duct.

The second component of velocity perpendicular to the magnetic field must also be calculated. An expression for this can be found by integrating eq. (14) along a magnetic field line

$$\int \mathrm{d}l\,\nabla\cdot\boldsymbol{v} = 0. \tag{22}$$

This results in an equation relating the required velocity component to the axial velocity component.

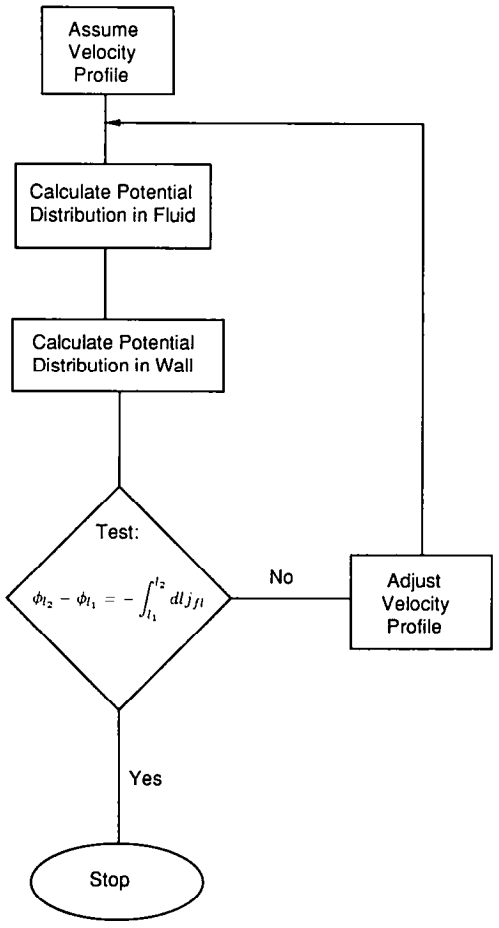

Fig. 1. Overview of the iterative solution method.

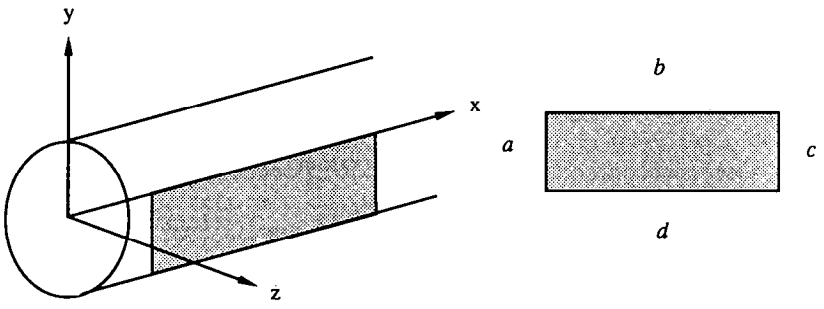

$\mathbf{B} = B\,(x)\,\mathbf{z}$

Fig. 2. Coordinate system and solution plane in the fluid.

After calculating a new velocity distribution, the potential in the fluid can be calculated again. This process is repeated until the criterion based on the potential variation along the field lines is satisfied. Fig. 1 gives a summary of the iterative procedure.

4. Application

The iterative solution method has been used to analyze flow in a straight, circular conducting duct, in the presence of a transverse magnetic field which can vary in the flow direction.

4.1. Equations and boundary conditions

Fig. 2 shows the plane in the fluid on which eq. (15) is solved, taking advantage of symmetry. In component form, using the coordinate system shown in fig. 2, after putting derivatives in terms of x and y only, this equation is

$$\frac{\partial^2\phi}{\partial x^2} + \frac{1}{B}\frac{\partial B}{\partial x}\frac{\partial \phi}{\partial x} + \frac{\partial^2\phi}{\partial y^2} = -B\frac{\partial v_x}{\partial y} + B\frac{\partial v_y}{\partial x} + 2v_y\frac{\partial B}{\partial x}. \tag{23}$$

After assuming a velocity profile, eq. (23) can be solved subject to the proper boundary conditions. At boundaries a and c, fully developed conditions are applied

$$\frac{\partial \phi}{\partial x} = 0. \tag{24}$$

At boundary b, due to symmetry

$$\phi = 0. \tag{25}$$

At boundary d, the thin-wall boundary condition is

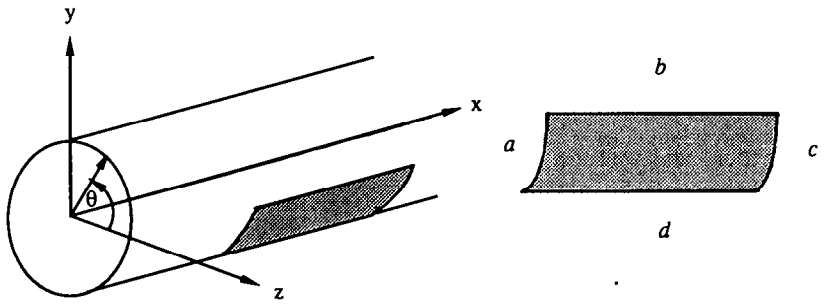

$\mathbf{B} = B\,(x)\,\mathbf{z}$

Fig. 3. Solution surface in the wall.

applied [5]

$$j \cdot n = \Phi \nabla_w^2 \phi, \tag{26}$$

where ∇_w^2 is the Laplacian in the wall only, and Φ is the wall conductance ratio, $\Phi = (\sigma_w t_w)/(\sigma_f a)$. This boundary condition enforces current conservation across the fluid–wall interface.

The x and y components of the current density can be calculated from Ohm's law (eq. (12)) once the potential distribution has been calculated.

In component form, based on the coordinate system shown in fig. 3, the equation for the potential distribution in the wall is

$$\frac{\partial^2 \phi}{\partial \theta^2} + \frac{\partial^2 \phi}{\partial x^2} = \frac{1}{\Phi}\left(-j_{fy} \sin\theta - \frac{1}{B}\frac{\partial B}{\partial x} j_{fx} z \cos\theta\right). \tag{27}$$

Eq. (27) can be solved subject to the correct boundary conditions. Fig. 3 shows the surface on which eq. (27) is solved, again taking advantage of symmetry. At boundaries a and c, fully developed conditions are applied

$$\frac{\partial \phi}{\partial x} = 0. \tag{28}$$

At boundary b, due to symmetry

$$\phi = 0. \tag{29}$$

At boundary d, due to symmetry

$$\frac{\partial \phi}{\partial \theta} = 0. \tag{30}$$

4.2. Convergence criterion

The z component of Ohm's law is integrated along a field line in order to determine the correct variation of the potential along field lines

$$\int_{z_1}^{z_2} \mathrm{d}z j_{fz} = -\int_{z_1}^{z_2} \mathrm{d}z \frac{\partial \phi}{\partial z}. \tag{31}$$

Substituting the expression for j_{fz} yields

$$\int_{z_1}^{z_2} \mathrm{d}z \frac{\partial \phi}{\partial z} = -\int_{z_1}^{z_2} \mathrm{d}z \frac{1}{B}\frac{\partial B}{\partial x} j_{fx} z. \tag{32}$$

Carrying out the integration results in

$$\phi(z_2) - \phi(z_1) = -\frac{1}{B}\frac{\partial B}{\partial x} j_{fx}\left(\frac{z_2^2}{2} - \frac{z_1^2}{2}\right). \tag{33}$$

If z_1 is evaluated at $z = 0$ and z_2 is evaluated at the wall, then

$$\phi_f - \phi_w = \frac{1}{B}\frac{\partial B}{\partial x} j_{fx}\frac{z_w^2}{2}. \tag{34}$$

If this criterion has not been met, the velocities must be adjusted.

4.3. Updating velocities

A new velocity distribution is calculated using Ohm's law

$$v_x^{new} = \frac{1}{B}\left(-\frac{\partial \phi_f^{new}}{\partial y} - j_{fy}^{old}\right), \tag{35}$$

where j_{fy}^{old} is the most recently calculated value. In this equation, ϕ_f^{new} is the result of taking a linear combination of the old potential, ϕ_f^{old}, and a new wall potential, ϕ_w^{new}, calculated using eq. (34)

$$\phi_f^{new} = \phi_f^{old}\rho_1 + \left(\phi_w^{old} + \frac{1}{2B} j_{fx}^{old}\frac{\partial B}{\partial x} z^2\right)\rho_2. \tag{36}$$

This velocity is normalized to satisfy global mass conservation using eq. (21). The variation of v_x along z can be found by taking the curl of Ohm's law and integrating, so the integration with respect to z in eq. (21) can be carried out to yield

$$\int \mathrm{d}y\left(v_{x0} z + \frac{1}{6B^2}\frac{\partial B}{\partial x}\frac{\partial j_x}{\partial y} z^3\right) = \text{constant}, \tag{37}$$

where $v_{x0} = v_x$ evaluated at $z = 0$.

An expression for the y-component of the velocity is found by using eq. (22)

$$\int \mathrm{d}z \frac{\partial v_x}{\partial x} + \int \mathrm{d}z \frac{\partial v_y}{\partial y} + \int \mathrm{d}z \frac{\partial v_z}{\partial z} = 0. \tag{38}$$

The third term can be integrated immediately

$$\int_0^{z_w} \mathrm{d}z \frac{\partial v_z}{\partial z} = v_{zz_w} - v_{z0}, \tag{39}$$

where z_w is the value of z at the wall.

It is necessary that there be zero mass flux into the wall. This implies

$$v_{zz_w} = -v_{yz_w} \tan\theta \tag{40}$$

at the wall. Due to symmetry, $v_{z0} = 0$.

Carrying out the integration yields

$$v_y = \frac{1}{z_w}\int \mathrm{d}y z_w \left(-\frac{\partial v_{x0}}{\partial x} + \frac{z_w^2}{6B^3}\left(\frac{\partial B}{\partial x}\right)^2 \frac{\partial j_x}{\partial y} - \frac{z_w}{2B^2} j_x \frac{\partial^2 B}{\partial x^2} \tan\theta - \frac{z_w}{2B^2}\frac{\partial B}{\partial x}\frac{\partial j_x}{\partial x}\tan\theta + \frac{z_w}{2B^3} j_x \left(\frac{\partial B}{\partial x}\right)^2 \tan\theta \right). \quad (41)$$

5. Benchmarking and results

A computer code was written and benchmarked using experimental results from ALEX (Argonne Liquid Metal Experiment) for flow in a conducting circular duct [6]. In particular, comparison of potentials, velocities, pressure gradients, and pressure differences were made in the region where the fluid exits the magnetic field. Only two of these comparisons are shown for space limitation reasons. All variables are presented in dimensionless form. The magnetic field variation at the exit of the field is shown in fig. 4. Figs. 5 and 6 show comparisons of the pressure gradients at $y = 1$ and the velocity profiles near $x = 0$, respectively. The pressure gradient was measured at $M = 10525$ and $N = 6541$. The velocity profile was measured at $M = 10000$ and $N = 6400$. There is a slightly larger bump in the pressure gradient near $x = 0$ in the code prediction than in the experimental data. This is because the pressure gradient in the experiment was measured over a 6-in. interval. This will smooth out the pressure gradient somewhat. Fig. 6 clearly shows the M-shaped velocity profile characteristic of flow in a nonuniform field. As can be seen, there is good agreement between the code results and the experimental results.

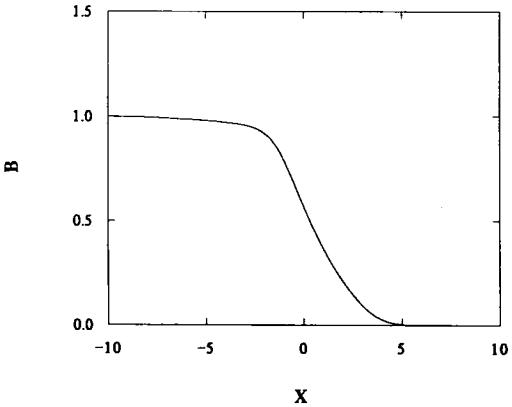

Fig. 4. Magnetic field variation at the exit of ALEX.

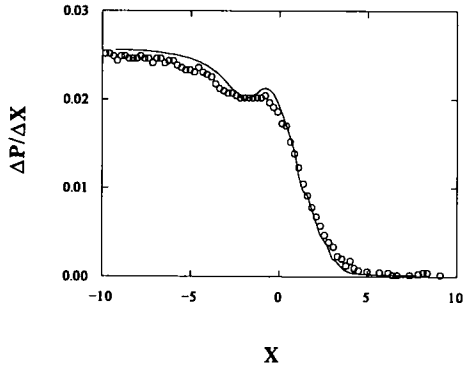

Fig. 5. Comparison of code prediction of the pressure gradient with experimental data from ALEX.

The code was used to analyze ducts with various wall conductivities and field variations in order to investigate their effect on the pressure gradient due to the varying field. This pressure drop occurs as a result of the longitudinal currents generated by a longitudinal potential gradient. This potential gradient is due to the variation of the quantity $v \times B$ (in this problem, B is varying). A similar result would occur due to a variation in cross-section, this time due to a change in v. The pressure drop due to the variation in the magnetic field can be calculated in the following manner. The computer code is used to calculate the total pressure drop,

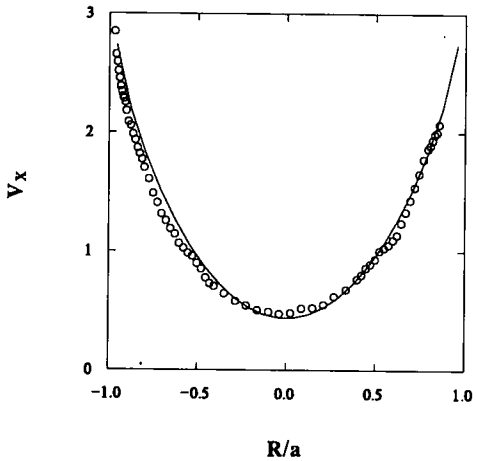

Fig. 6. Comparison of code prediction of the velocity profile near $x = 0$ with experimental data from ALEX.

and the fully-developed flow pressure drop is then subtracted

$$\Delta p_{\text{field variation}} = \Delta p_{\text{code}} - \frac{\Phi}{1+\Phi}\int_0^x \mathrm{d}x B^2. \qquad (42)$$

Fig. 7 shows how the value of the pressure drop for $\Phi = 0.03$ and $\Phi = 0.30$ varies as a function of B_2. In these calculations, the field was assumed to vary linearly from $B = 1.0$ to $B = B_2$ over a distance of 5.25 duct radii. The pressure drop is greatest for the largest change in B. This is expected, since the larger the change in B, the greater the longitudinal potential gradient which implies larger currents, and hence a greater pressure drop. Although the magnitude of the pressure drop is less for $\Phi = 0.03$ than $\Phi = 0.30$, the pressure drop with the lower value of Φ is greater relative to the straight duct pressure drop. The pressure drop due to the varying field becomes more significant as Φ decreases.

Fig. 8 shows the effect the distance over which the field changes has on the pressure drop due to the varying field. Results are shown for ducts with $\Phi = 0.03$ and $\Phi = 0.30$, with the field varying linearly from 1.0 to 0.5 over distances from $0.5a$ to $10a$. The greatest pressure drop occurs for the more quickly varying field for the same reasons as given in the previous paragraph. Again, the varying field pressure drop relative to the fully developed flow pressure drop is greater for the duct with the lower wall conductance ratio.

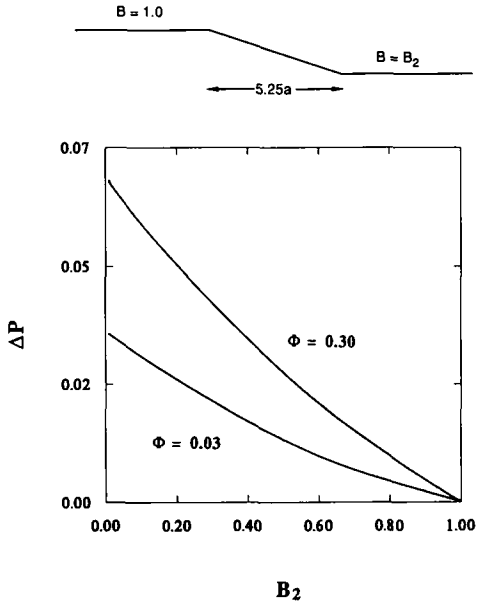

Fig. 7. Pressure drop due to varying field as a function of B_2.

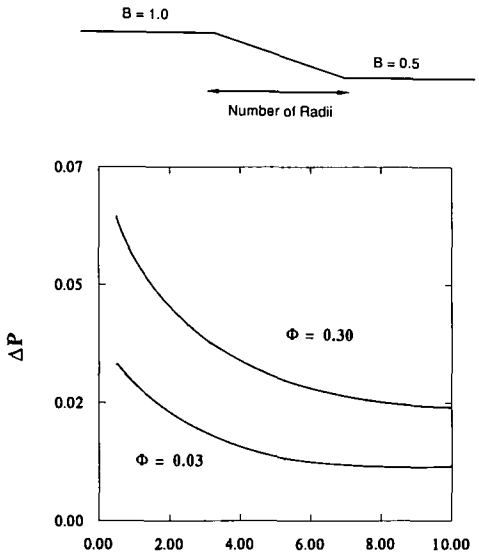

Fig. 8. Pressure drop due to varying field as a function of distance over which the field varies.

6. Conclusions

The core flow approximation is a powerful tool for analyzing MHD flow at high M and N. It gives an accurate prediction of the MHD fluid flow. The iterative method has been used to analyze a problem with simple geometry. In order to determine the potential of this method, it is necessary to use it to evaluate a more complicted geometry such as a multiple duct problem. In addition, determination of the ranges over which the core flow approximation method is applicable should be done.

Nomenclature

a	duct half-width,
$\boldsymbol{B}$	magnetic field,
$\boldsymbol{j}$	electric current density,
$\boldsymbol{n}$	unit normal,
p	pressure,
t_w	wall thickness,
$\boldsymbol{v}$	velocity,

x, y, z cartesian coordinates,
θ angle measured with respect to positive z axis,
μ viscosity,
ρ fluid density,
σ electric conductivity,
ϕ electric potential,
Φ wall conductance ratio.

References

[1] R.J. Holroyd and J.S. Walker, A theoretical study of the effects of wall conductivity, non-uniform magnetic fields and variable-area ducts on liquid-metal flows at high Hartmann number, J. Fluid Mech. 84 (1978) 471.

[2] C.B. Reed, B.F. Picologlou, T.Q. Hua and J.S. Walker, ALEX results – a comparison of measurements from a round and rectangular duct with 3-D code predictions, presented at the IEEE 12th Symp. on Fusion Engineering, Monterey, CA (October 1987), to be published in Fusion Technology.

[3] M.S. Tillack, Core flow solution of the liquid metal MHD equations in a variable-radius pipe, UCLA-ENG-87-27 (July 1987).

[4] J.C.R. Hunt and R.J. Holroyd, Applications of laboratory and theoretical MHD duct flow studies in fusion reactor technology, Culham Laboratory Report, CLM-R-169 (May 1977).

[5] J.A. Shercliff, The Theory of Electromagnetic Flow Measurement (Cambridge University Press, 1962), p. 27.

[6] B.F. Picologlou, C.B. Reed and P.V. Dauzvardis, Experimental and analytical investigations of magnetohydrodynamic flows near the entrance to a strong magnetic field, Fusion Technol., 10 (1986).